Distributed Classifier Based on Genetically Engineered Bacterial Cell Cultures

Andriy Didovyk,[†] Oleg I. Kanakov,[∥] Mikhail V. Ivanchenko,[⊥] Jeff Hasty,[†,‡,§] Ramón Huerta,*[,†] and Lev Tsimring*[,†]

[†]BioCircuits Institute, [‡]Department of Bioengineering, [§]Molecular Biology Section, Division of Biological Science, University of California San Diego, La Jolla, California 92093, United States

[∥]Department of Radiophysics, [⊥]Department for Bioinformatics, Lobachevsky State University of Nizhniy Novgorod, Nizhniy Novgorod, Russia

S *Supporting Information*

ABSTRACT: We describe a conceptual design of a distributed classifier formed by a population of genetically engineered microbial cells. The central idea is to create a complex classifier from a population of weak or simple classifiers. We create a master population of cells with randomized synthetic biosensor circuits that have a broad range of sensitivities toward chemical signals of interest that form the input vectors subject to classification. The randomized sensitivities are achieved by constructing a library of synthetic gene circuits with randomized control sequences (e.g., ribosome-binding sites) in the front element. The training procedure consists in reshaping of the master population in such a way that it collectively responds to the "positive" patterns of input signals by producing above-threshold output (e.g., fluorescent signal), and below-threshold output in case of the "negative" patterns. The population reshaping is achieved by presenting sequential examples and pruning the population using either graded selection/counterselection or by fluorescence-activated cell sorting (FACS). We demonstrate the feasibility of experimental implementation of such system computationally using a realistic model of the synthetic sensing gene circuits.

KEYWORDS: *chemical pattern recognition, consensus classification, distributed sensing, machine learning, microbial population engineering, synthetic circuits*
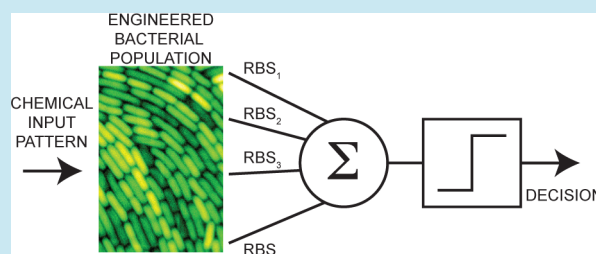
Pattern recognition and classification is one of the most important statistical disciplines.[1] Its applications span across disciplines such as computer vision,[2] natural language processing,[3] search engines,[4] medical diagnosis,[5] classification of DNA sequences,[6] speech recognition,[7] computational finance,[8] fraud detection,[9] and many others.[10] In these contexts usually a system that solves a pattern recognition problem learns from the "training" data presented to it. Using the "training" data, such a system forms an internal model to classify new previously unseen data. Typically these models are built in regular computers, although alternative approaches have been proposed.[11,12]

Many pattern recognition algorithms are biologically motivated. Biological organisms perform decision making based on classification of external environmental cues at all levels from intracellular (e.g., ref 13) to organismal[14] and even population-wide.[15] The development of artificial neural network (ANN) classifiers was inspired by the brain's natural ability to perform complex computational and classification tasks.[16] The main principles of brain dynamics, its layered organization and ability to learn by adapting strengths of interneuron synaptic connections (plasticity) is mimicked in ANN by multilayered perceptrons and various learning algorithms.[17]

A different learning approach is motivated by the adaptive immune system of jawed vertebrates, which employs a population of lymphocytes (T and B cells) with a diverse genetically encoded library of recognition specificities in order to implement learning, memory, and pattern recognition capabilities.[18,19] Lymphocytes with different receptor variants undergo essentially a supervised learning procedure in central lymphoid organs, being presented self-antigens as examples. Positive selection retains T cells capable of interacting with the major histocompatibility complex while negative selection eliminates self-reactive T and B cells. Subsequent exposure of mature lymphocytes to foreign antigens results in positive selection of the reactive clones. The adaptive immunity classifier is not a single complex multivariate system with parameters adjusted in course of learning. Rather, it is a distributed system that consists of a large number of relatively simple cellular classifiers and implements learning through deletion of outliers. When trained, it solves a consensus classification problem, reporting the absence of pathogens if

and only if each cellular classifier does not respond to presented antigens. The main principles of the natural adaptive immune system of jawed vertebrates have inspired the branch of computer science known as Artificial Immune Systems (AIS).[20−22]

In this work, we propose to use synthetic biology to adapt biological systems themselves for solving complex classification tasks. While the most straightforward solution for this problem would be to design a single gene circuit that would produce output signal sufficient for classification, in practice, the uncertainty and wide dynamic range of possible signals of interest would render this solution suboptimal. In such situations, it appears useful to borrow the principles underlying the distributed classification abilities of natural adaptive immune system and create a heterogeneous population of microorganisms with different synthetic gene circuits capable of performing classification tasks based on consensus strategy. The desired binary classifier should produce a positive response (for example, above-threshold population-averaged fluorescence level) to positive inputs and negative response (below-threshold fluorescence) to negative ones. The learning algorithm then should consist of shaping the population in such a way that the population collectively "arrives" at a probably correct decision.

The idea of aggregating many simple classifiers to yield a better classifier is a widely used strategy in machine learning that capitalizes on the idea that using a set of classifiers that produce barely better results than random guessing can achieve arbitrarily high accuracy when combined appropriately.[23] It also can be cast as a function approximation problem in which a complex target function is approximated by a weighted sum of multiple simpler functions, such as radial basis functions[24] or wavelets.[25] Inspired by these ideas, we propose to use genetically engineered cells with limited abilities to perform complex classification tasks.

Here, we present a specific biological implementation of this general distributed pattern recognition system concept using a model of synthetic gene regulatory circuits in engineered cell populations. The proposed implementation requires to build a cell library with genetically encoded randomized sensitivities to external chemical signals to be classified. Such libraries have been successfully constructed for optimization of synthetic biological circuits.[26−28] One could in principle envision a system in which different strains were placed in different chambers and probed separately, and then, the classification task would be done *in silico*. However, this approach would entail a complex multichamber, multichannel system that would be difficult to operate in an open environment. Instead, we propose here to use a library to form a *master classifier* population that is pruned to learn how to solve a certain classification task. In the properly trained system, classification is based on a single population-averaged output, which simplifies the device design and operation considerably. The learning is done by examples: cells with erroneous outputs are gradually attenuated from the population, while the "correct" cells are amplified. As a result of multiple iterations of pruning/amplification, a distributed classifier trained for a specific task emerges from the master population. We envision that an arbitrary external input subject to recognition can be encoded by a combination of chemical inputs capable of generating the engineered cellular response. In this paper, however, we will consider the most straightforward case when the vector of chemical concentrations *is* the input signal subject to

classification. In the following, we demonstrate the general principle of this classification procedure and describe its implementation using a model of a synthetic genetic circuit based on the lambda phage P_{RM} promoter.[13]

■ RESULTS AND DISCUSSION

Learning by Examples. In this section, we describe the general idea behind the training of a distributed classifier by presenting a set of positive and negative examples. In the following, we denote the set of input variables to be classified as $\mathbf{x} \in \mathcal{R}^M$. A classifier is the function $y = 2H\left(f(\mathbf{x}) - \theta\right) - 1$, such that if $f(\mathbf{x}) > \theta$, the answer is $y = 1$, and otherwise, $y = -1$. Here $H(\cdot)$ is the Heaviside function, θ is a scalar threshold, and $f(\mathbf{x})$ is the scalar function of the inputs. The heart of the pattern classifier is the function $f(\mathbf{x})$ that minimizes the classification errors for a given distribution of positive and negative inputs.

In general, the classifier function is not known *a priori* and has to be learned by training the classifier using examples (training data). The training of a classifier by examples consists in finding a function $f(\mathbf{x})$ that minimizes the error in mapping of a given set of N examples $\mathbf{x}_i$ to a set of binary outputs, $y_i = \{-1,+1\}$ which label the examples. In the following, we will say that if the output $y_i = +1$, the example i belongs to the "positive" class and if the output is $y_i = -1$ the example i belongs to the opposing "negative" class.

In our proposed population-based classifier, $\mathbf{x}$ will be a set of concentrations of chemical signals to which cells are subjected, and the cells are assumed to contain gene circuits that produce a fluorescent signal $z_i(\mathbf{x})$ in response to the input signal $\mathbf{x}$. The overall signal function, $f(\cdot)$, will be the normalized linear sum of the individual fluorescence signals from all N_c cells in the trained population:

$$f(\mathbf{x}) = \frac{1}{N_c} \sum_{i=1}^{N_c} z_i(\mathbf{x}) \tag{1}$$

The key to the "trainability" of the distributed classifier is to prepare a master population of cells with broadly varied functions $z_i(\mathbf{x})$, so this population can be appropriately shaped to perform the needed classification task. This can be achieved using synthetic gene regulatory circuits with randomized control elements such as promoter regions, ribosome binding sites, or other sequences as described in detail below.

We assume that the master population contains cells that individually provide correct answers to subsets of the data to be classified but that, in general, no single cell provides correct answers to all data (weak classifiers). The goal of training is therefore to shape the master population to create a distributed consensus classifier that performs better then any cell individually. Such training must amplify the cells providing correct answers as frequently as possible and conversely suppress the cells with poor overall performance. Thus, our proposed learning procedure consists in modifying the composition of the cell population based on the examples with known outcomes. The details of our training algorithm for the specific implementation of a genetic sensing circuit are outlined below.

Distributed Classification with Randomized Synthetic Gene Sensors. Here, we outline an implementation of the proposed distributed classifier with a diverse population of bacterial cells containing synthetic sensory genetic circuits with randomized parameters. For simplicity we focus on a scalar input with only one chemical signal affecting the gene circuit,

however, the same approach can be straightforwardly generalized to the multidimensional vector input. In our two-gene design (Figure 1), the sensing and the reporting
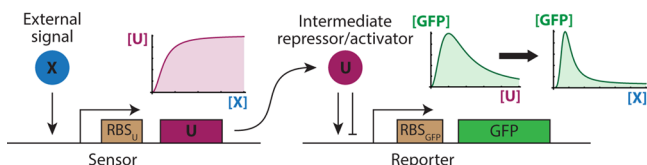
Figure 1. Modular genetic circuit proposed for implementing a distributed genetic classifier. Sensing and response functionalities are split into separate modules. In the first module (sensor), an inducible promoter drives the expression of the transcription factor U in response to the applied signaling molecule X. The response function of the promoter is chosen to be monotonic (see inset). In the second module (reporter), another inducible promoter drives the expression of a reporter (GFP) in response to induction by U. The promoter is activated by intermediate concentrations of U and inhibited by high concentrations of U. Thus, the resulting response function of the entire two-promoter circuit to the concentration of signaling molecule is bell-shaped for the relevant values of the circuit parameters as shown on the inset.

functionalities are split between the two genetic modules. The sensing module is monotonically induced by the external chemical signal X and drives the synthesis of a transcription factor U. The second promoter is regulated by U and drives the expression of a reporter protein, for example, green fluorescent protein (GFP). The reporter promoter is activated by U at intermediate concentrations and inhibited at higher concentrations, thus being active only within a finite range of concentrations of U. The classic well-characterized example of such promoter is the promoter P_{RM} of phage lambda, which is activated by intermediate concentrations and is repressed by high concentrations of the lambda repressor protein CI.[13,29]

This two-gene circuit can be modeled by the following set of biochemical reactions

$$\emptyset \xrightarrow{r_u(x)} U; \qquad U \xrightarrow{\mu_u} \emptyset$$

$$\emptyset \xrightarrow{r_g(u)} GFP; \qquad GFP \xrightarrow{\mu_g} \emptyset$$
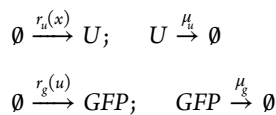
where x and u are the concentrations of X and U, $r_u(x)$ and $r_g(u)$ are the effective production rates of U and GFP, respectively, and μ_u and μ_g are the degradation rates of U and GFP. The rates of gene expression in this system can be described by standard Hill functions:

$$r_u(x; m_u) = m_u \frac{\alpha A_u^{p_u} + x^{p_u}}{A_u^{p_u} + x^{p_u}} \tag{2}$$

$$r_g(u; m_g) = m_g \frac{A_g^{p_g} u^{p_g}}{(A_g^{p_g} + u^{p_g})^2} \tag{3}$$

where α describes the basal expression from the sensor promoter in the absence of the signaling molecule X, A_u is the dissociation constant of X with the sensor promoter, the Hill coefficient p_u characterizes the cooperativity of activation of the sensor promoter, p_g characterizes the cooperativity of activation and repression of the reporter promoter by the transcription factor U, A_g is the dissociation constant for activation and repression of the reporter promoter by U (we assume the activation and repression cooperativities and dissociation

constants to be the same), m_u and m_g describe the overall strength of production of U and GFP, respectively. Noteworthy, such Hill functions based model provides a simple yet adequate approximation of more complex response functions required to describe real promoters[29] (see Supporting Information Section 3).

In mass-action approximation the dynamics of GFP production in this system is described by the following system of ordinary differential equations:
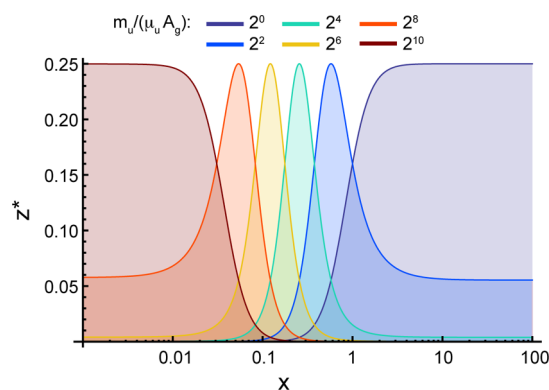
$$\frac{du}{dt} = r_u(x; m_u) - \mu_u u \tag{4}$$

$$\frac{dz}{dt} = r_g(u; m_g) - \mu_g z \tag{5}$$

where z is the concentration of GFP. The steady state concentration of GFP as a function of the concentration of the external chemical signal X can be found from the eqs 4 and 5 as

$$z^*(x; m_u, m_g) = \frac{r_g(r_u(x; m_u)/\mu_u; m_g)}{\mu_g} \tag{6}$$

The function $z^*(x)$ is bell-shaped in a broad range of $m_u/\mu_u \in (A_g, A_g/\alpha)$ (Figure 2). Varying m_u/μ_u allows to create a library of

Figure 2. Steady state GFP concentration (z^*) as a function of the concentration of the external chemical signal X for the modular classifier circuit shown for a range of m_u values representing a range of the relative strengths of the sensor promoter (Figure 1). Nondimensional circuit parameters are $\mu_u = \mu_g = m_g = A_u = 1$, $A_g = 20$, $p_g = p_u = 2$, $\alpha = 10^{-3}$.

circuits which act as low-pass filters ($m_u/\mu_u \leq A_g$), high-pass filters ($m_u/\mu_u \geq A_g/\alpha$), or tunable bandpass filters for the intermediate values of m_u/μ_u. As described in the following sections, such a library can be used to train a cell population-based distributed classifier. Since common sensor promoters can have a regulatory range of over 10^3 ($\alpha = 10^{-3}$),[30,31] to create a library that contains low-pass, bandpass, and high-pass filters, the m_u/μ_u ratio has to be varied at least $1/\alpha = 10^3$ fold within $[A_g, A_g/\alpha]$ range (see Figure 2). Such libraries have been widely constructed experimentally: m_u can be varied over more than 10^5 fold range by varying the DNA sequence within and near the ribosome binding site of the gene of interest;[32,33] this range can be further expanded by modulating the sensor promoter strength;[34] m_u/μ_u ratio can also be modulated by varying the stability of the U coding mRNA as well as the stability of the protein U itself.[26,35−37]

The modular architecture of the classifier circuit proposed here allows us to independently select and optimize the sensor

and the reporter functionalities in order to maximize the classifier performance. Well-characterized sensor promoters, which can be induced by a variety of chemical signals with the appropriate monotonic response, are common[30,31,38−40] and can be readily combined with the reporter promoter such as the well characterized lambda phage promoter P_{RM}.[13,29] For these reasons the proposed two-gene sensory circuit appears to be well-suited for experimental implementation of a distributed cell population based classifier.

Classifier Training Algorithm. In order to train a classifier we need to be able to sort individual cells based on their response to a set of known examples. A hard-decision algorithm implies that if a given example x_i belongs to a positive class, $y_i = +1$, and the GFP level in j-th cell is above a threshold $z_j^*(x_i) > \theta$, then that particular cell should be retained in the population because the cell provides the correct answer. Meanwhile, the cells not reaching the threshold expression level after presenting a positive example should be removed from the population. On the other hand, if a negative example is presented ($y_i = -1$), the cells generating above-threshold fluorescence should be eliminated and the cells that are below threshold should be retained. By this selection mechanism, we ensure that only the cells generating correct answers survive.

However, this hard-decision training algorithm in most practical situations leads to poor performance. As mentioned above, in general, each cell is a weak classifier and so it cannot provide the complete classification solution. If positive and/or negative categories encompass a broad range or several distinct ranges of inputs, a subpopulation in which all cells generate above-threshold output for positive examples and below-threshold output for negative examples would be empty. Thus, an outright elimination of all cells producing "incorrect answer" to any of many training examples would eventually lead to elimination of all cells. To avoid this undesirable outcome, a "soft-training" algorithm has to be employed in which even the "erroneous" cells have a chance to remain in the population, and so the resultant population-based classifier will produce the correct answer only by the population average, not the unanimous decision of all cells.

We postulate that the elimination of cells from the population is governed by two sigmoidal cell survival probability functions $p_+ (z_j^*) = (1 + \xi)^{-1} + (1 + \xi \exp(-z_j^*/\gamma))^{-1}$ and $p_- (z_j^*) = 1 + (1 + \xi)^{-1} - (1 + \xi \exp(-z_j^*/\gamma))^{-1}$ for positive and negative examples correspondingly, where $\xi = \exp((8\gamma)^{-1})$ and $0 \leq z_j^* \leq {}^1/_4$ are chosen to encompass the entire range of possible values of z_j (eq 6) (Figure 3). These functions are chosen such that the cells that respond perfectly to the presented example ($z_j^* = {}^1/_4$ or $z_j^* = 0$ for a positive or a negative example correspondingly) are retained in the population ($p_\pm (z_j^*) = 1$). Otherwise the cells are eliminated
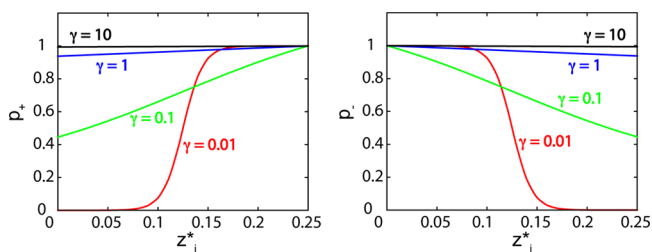
Figure 3. Cell survival probabilities during training upon presentation of a positive ($p_+ (z_j^*; \gamma)$) or a negative example ($p_- (z_j^*; \gamma)$).

from the population with a probability that depends on the cell fluorescence z_j^* and the "rigidity" of training γ. For very small γ, cells not responding to the currently presented input are eliminated with high probability. This can potentially eliminate many cells required to recognize other positive examples x_i from the pattern being taught leading to the poor overall performance. For too large γ (weak elimination), the learning rate slows down significantly requiring unreasonably large number of training iterations in order to achieve high performance. Therefore, an optimal value of the parameter γ can be chosen to balance performance with the learning speed. In general, this value will be different for each individual problem. Experimentally these selection functions can be implemented via fluorescence activated cell sorting (FACS) or well established genetically encoded positive/negative selection systems.[41] Conveniently, in the latter case positive or negative example is indicated by applying the corresponding selective compound to the cells and its concentration can be used to adjust the rigidity of training (γ).

As usual in the design of classifiers, the output element of the classifier must be a threshold element. In the distributed classifier described here, the mean population fluorescence $f(x)$ has to be compared with a suitably chosen threshold θ such that the above-threshold fluorescence ($f(x) > \theta$) corresponds to the positive class, and below-threshold fluorescence ($f(x) < \theta$) to the negative class. The optimal threshold θ can be found by presenting the training set of examples and minimizing the percentage of incorrect answers. The training procedure described above can be formalized as Algorithm 1 (Figure 4).

Input: The data set x_i with N examples. The class type y_i for each example. The total number of cells N_c. The number of iterations of the algorithm, N_{iter}.
Output: The trained set consisting of N_c selected cells; classification threshold θ.
for iteration $k \leftarrow 1$ to N_{iter} **do**
  Choose a random example from x_i in the range $i = 1, \dots, N$ {Apply the chosen chemical input to the cells.}
  for $j \leftarrow 1$ to N_c **do**
    Eliminate the cell with probability $1 - p_\pm(z_j^*(x_k))$ (for $y_i = \pm 1$) with random cell replacement from the previous iteration or from the master population for $k = 1$.
  end for
end for
for training example $i \leftarrow 1$ to N **do**
  Use selected cells to measure the mean population fluorescence:
  $f(x_i) \leftarrow N_c^{-1} \sum_{j=1}^{N_c} z_j(x_i)$
end for
Find threshold θ for which $\sum_{k=1}^{N} y_k [2H(f(x_k) - \theta) - 1]$ is maximal

---

Figure 4. Algorithm 1: Algorithm for training the gene expression classifier.

In the following sections we use this algorithm to train a computational model of the distributed gene expression classifier and analyze its performance using sets of simulated data. We generate these sets using the model of the synthetic gene circuit (eq 6) presented above. In order to simulate the combined effects of biological and instrumental noise on the performance of the classifier we will assume that the resultant mean fluorescence of the population contains both additive and multiplicative noise:

$$f(x) = \frac{1}{N_c} \sum_{i=1}^{N_c} z_i(x)(1 + \varepsilon) + \zeta \tag{7}$$

where ε and ζ are independent normal random variables with the respective means of 0 and $\sigma/4$ and standard deviations σ and $\sigma/4$. As usual in performance evaluation, each data set is divided into two parts, one for training and another for testing, and the overall performance of the classifier is measured as the

percentage of correct answers on the test sets. The classifier performance is calculated using Algorithm 2 (Figure 5).


Input: The testing data set x_i with N examples. The class type y_i for each example. The total number of cells N_c.
Output: The performance of the classifier.
Use all the cells selected during training.
correct $\leftarrow 0$
for $i \leftarrow 1$ to N **do**
   Measure average population fluorescence $f(x_i)$
   if $f(x_i) > \theta$ and $y_i = 1$ **then**
     correct=correct+1
   end if
   if $f(x_i) < \theta$ and $y_i = -1$ **then**
     correct=correct+1
   end if
end for
performance=correct/N

**Figure 5.** Algorithm 2: Algorithm for testing the gene expression classifier.

Classification Problems. Before we present our numerical results demonstrating the performance of the distributed classifier, let us discuss the motivation for using nonseparable data sets as representative examples of real world classification problems. If the classes were completely separated, then a properly trained classifier would be able to identify the boundary (or a manifold in a multidimensional input space) between the classes and perform classification with 100% accuracy. However, in reality different classes often overlap, and therefore 100% accuracy of classification cannot be attained. Real-world biological and medical data frequently consists of overlapping (nonseparable) classes.[42,43] To illustrate how nonseparable classes can emerge even in a simple biochemical system, we consider an example of two toxins that additively contribute to the overall toxic effect on the cells. In such case, in a two-dimensional plane of two toxin concentrations there exist a straight line where the overall toxicity is equal to a certain threshold;[44,45] thus, the positive and negative classes are separable (Figure 6A). For specificity, we define a positive class as a domain of concentrations of Toxin A and Toxin B, which cause less than 50% population mortality after a specified test duration; all other combinations of concentrations by definition are assigned to the negative class. Now, let us assume that the concentrations of both toxins are distributed according to some random distribution (e.g., log-normal), but our sensor can only
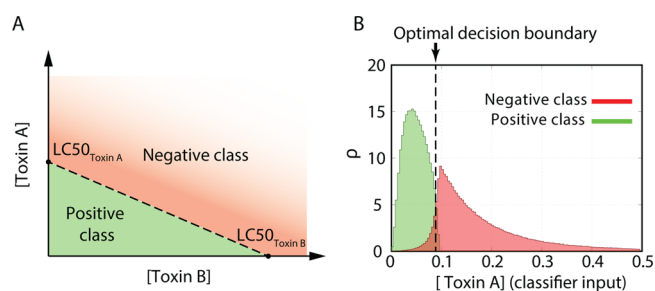
Figure 6. (A) Definition of positive and negative classes for two additively interacting toxins. (B) Positive and negative classes separable in two dimensions become nonseparable in one dimension, that is, when only the concentration of one of the toxins can be measured directly and the other becomes a hidden random variable. For illustrative purposes, we assumed log-normal distributions of toxin concentrations. A histogram of 10^6 examples is shown. Optimal decision boundary for a naive Bayes classifier is shown with a dashed line.

measure concentration of only one of the toxins (e.g., Toxin A). In this case, the two-dimensional positive and negative classes are projected onto Toxin A axis and become nonseparable (Figure 6B). The concentration of the unmeasured Toxin B becomes a hidden variable that makes positive and negative classes nonseparable. More generally, all the unknown or unmeasured environmental conditions can render two sets of measured conditions nonseparable. In such cases, the classification task consists of learning the optimal discrimination boundary along Toxin A axis that maximizes the discriminatory power of the classifier at the level below 100% accuracy. In the absence of *a priori* information about the known and unknown toxin distributions and their effect on cell viability, the optimal decision boundary will have to be inferred solely from random examples presented to the classifier, thus the performance of a real classifier will be even lower.

In order to clearly demonstrate the salient features of the classifier and study the limits of its performance, we will continue with two "idealized" classification problems. First, we consider the case of discriminating data generated by two log-normal distributions of input chemical concentration with some overlap between the two classes (Figure 7A). This example is
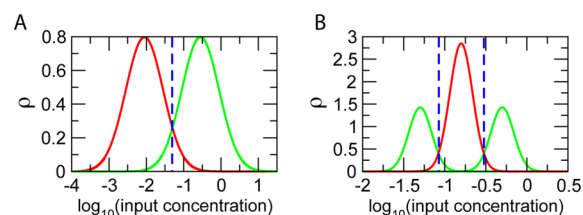
Figure 7. Data is generated from two (left) or three (right) log-normal distributions generating the positive class (green) and the negative class (red) examples. The optimal thresholds for discriminating between the classes are represented by the dashed vertical lines. The maximum performance achievable by a classifier trained on infinite amount of examples from the two distributions is 93.3%, from the three distributions is 94.8%. The minimum in both cases is 50% which is equivalent to a random answer selection.

qualitatively similar to the two-toxin example discussed above, except that there is a nonzero probability of having points far from the decision boundaries (it is a harder problem). After that, we test the distributed classifier on a more challenging problem of discriminating the data generated by complex distributions (one unimodal and another bimodal), when the negative class is surrounded by the positive class on both sides (Figure 7B).

Discrimination of Two Unimodal Classes. As the first example we used the data drawn from two log-normal distributions centered at $\log(x) = -0.55$ (class +1) and $\log(x) = -2.05$ (class −1) with standard deviation of 0.5 (Figure 7A). The data has been generated on a log-scale since it is the natural scale of the response of the genetic circuit used in the classifier (Figure 2). Figure 7A gives an illustration of the two generating distributions. The optimal theoretical performance is determined by choosing the threshold that separates the positive-class distribution from the negative one in a manner that minimizes discrimination errors. In this particular case, the optimal threshold value that leads to the minimal number of errors and therefore to the maximum performance is located exactly in the middle between the peaks of the two distributions which is indicated by the blue dashed vertical line ($\log(x) = -1.3$). Due to the nonseparability of the two classes, it is
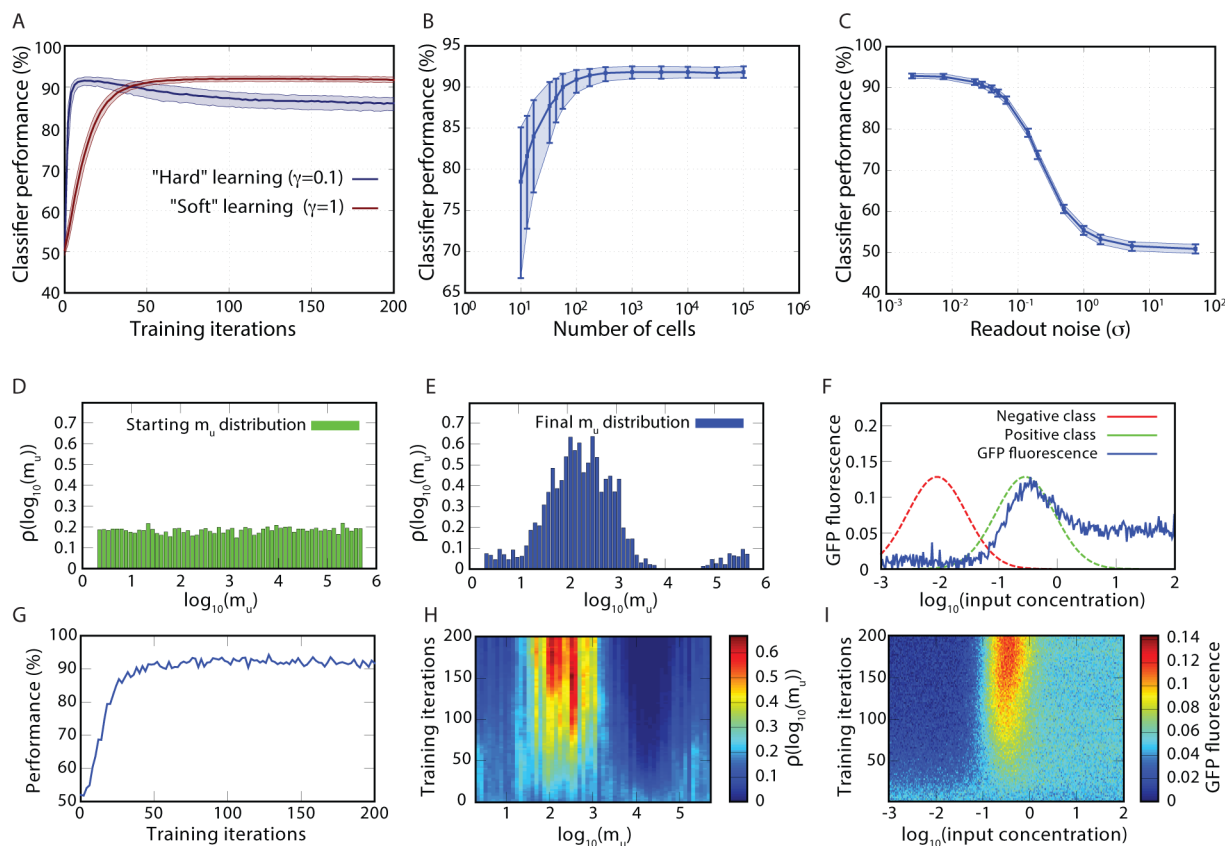
Figure 8. Classification results for the data set drawn from two unimodal classes, Figure 7A. (A) Evolution of the classifier performance for $\gamma = 0.1$ ("hard" learning; blue) and $\gamma = 1$ ("soft" learning; red), population size $N_c = 10^4$ cells. The classifier performance versus cell population size N_c (B) or GFP fluorescence readout noise σ (C); $\gamma = 1$ in (B) and (C), $N_c = 10^4$ in (C). The median and interquartile range of the distribution of the classifier performance calculated from 10^3 different stochastic realizations are shown in parts A−C, readout noise $\sigma = 1/35$ in A and B. (D−I) Evolution of the parameters of the classifier before and after training—an example trajectory. The parameters used are $\gamma = 1$, $N_c = 10^4$, $\sigma = 1/35$. It illustrates the shift in the distribution of parameters due to the training process of elimination of cells. The distribution of RBS/promoter strengths m_u before training (D) and after 200 training iterations (E). (F) Normalized GFP fluorescence of the ensemble of cells $f(x)$ (blue) after 200 training iterations, log-normal distributions generating positive (green) and negative (red) class examples. (G) Evolution of the classifier performance in this realization. Evolution of m_u distribution (H) and normalized cumulative GFP fluorescence $f(x)$ (I).

impossible to solve this classification problem with 100% success rate. The optimal theoretical performance for this problem is 93.3%. An ideal classifier could approach this value for infinite amount of training and evaluation data.

Using a "hard" learning strategy (small $\gamma = 0.1$), the population-based classifier achieves high performance of 91.6% in just 12 iterations; however, with further training the performance deteriorates achieving 86.1% after 200 iterations (Figure 8A). These results are obtained using $N_c = 10^4$ cells (all other circuit parameters are as described in Figure 2). Such deterioration of performance is a well-known phenomenon in machine learning, where early stopping is often applied in similar situations.[46,47]

In contrast, as discussed above, a "soft" learning strategy ($\gamma = 1.0$) allows one to achieve the maximum performance (92.0%) with high robustness over a wide range of training iterations (Figure 8A). Relatively small number of cells is sufficient to achieve such performance (Figure 8B). The classifier is also robust to readout noise (Figure 8C).

The evolution of the parameters of the classifier during "soft" training is demonstrated in Figure 8D−I. The training process leads to a robust selection of the cells with those values of the genetic diversity parameter m_u that allow the normalized population-wide GFP response $f(x)$ to roughly track the

positive class data distribution (Figure 8E−F, H−I). Correspondingly it is possible to reliably select such a threshold θ (Algorithm 2, Figure 5) that allows the classifier to achieve performance close to the theoretical maximum for this problem after roughly 50 training iterations (Figure 8G).

We also analyzed the performance of the distributed classifier on the more realistic unimodal example of dual-toxin cell viability classification with one toxin measured and another unobserved which was introduced in the beginning of this section (see Supporting Information Section 2). The classifier achieves high performance of about 95% after learning just 15 examples using "hard" ($\gamma = 0.1$) training strategy (Figure S3 of the Supporting Information).

Discrimination of a Bimodal and a Unimodal Class. This is a more challenging one-dimensional classification problem where a negative class is "sandwiched" by the positive class on both sides (Figure 7B). The negative class data is generated by a log-normal distribution centered at $\log(x) = -0.8$. The positive class data is generated from two equivalent log-normal distributions centered at $\log(x) = -1.3$ and -0.3. The standard deviation of all three distributions is 0.14. The distributions are normalized such that on average the equal number of examples is drawn from the negative and positive classes. The maximum theoretical performance on this problem
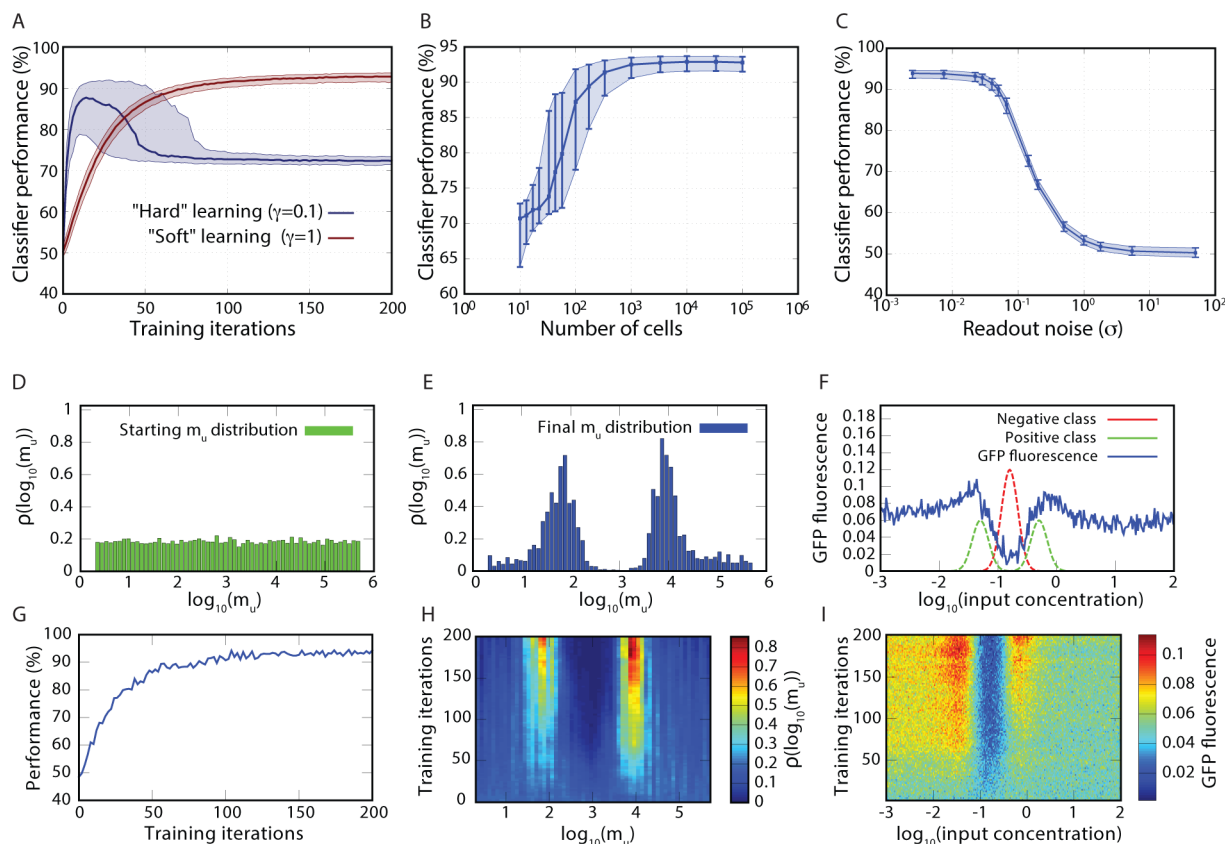
Figure 9. Classification results for the data set drawn from one bimodal and one unimodal classes, Figure 7B. (A) Evolution of the classifier performance for $\gamma = 0.1$ ("hard" learning; blue) and $\gamma = 1$ ("soft" learning; red), population size $N_c = 10^4$ cells. The classifier performance versus cell population size N_c (B) or GFP fluorescence readout noise σ (C); $\gamma = 1$ in (B) and (C), $N_c = 10^4$ in (C). The median and interquartile range of the distribution of the classifier performance calculated from 10^3 different stochastic realizations are shown in parts A−C, readout noise $\sigma = \frac{1}{35}$ in A and B. (D−I) Evolution of the parameters of the ensemble of cells before and after training−an example trajectory. The parameters used are $\gamma = 1$, $N_c = 10^4$, $\sigma = \frac{1}{35}$. It illustrates the shift in the distribution of parameters due to the training process of elimination of cells. The distribution of RBS/promoter strengths m_u before training (D) and after 200 training iterations (E). (F) Normalized GFP fluorescence of the ensemble of cells $f(x)$ (blue) after 200 training iterations, log-normal distribution generating positive (green) and negative (red) class examples. (G) Evolution of the classifier performance in this realization. Evolution of m_u distribution (H) and normalized cumulative GFP fluorescence $f(x)$ (I).

is 94.8%, determined as in the example above. We use the same genetic circuit parameters as in the previous example (see Figure 2).

This classification problem exemplifies the differences between the "hard" and "soft" learning strategies (Figure 9A). Similarly to the previous example the "hard" learning strategy ($\gamma = 0.1$) initially leads to rapid improvement of classifier performance, reaching the maximum performance of 87.7% in 14 iterations. However, unlike the previous example, this increase is not robust and is characterized by high stochastic variability (compare Figures 8A and 9A). With further training the performance quickly degrades due to stochastic extinction of the cells fitting one of the two positive class distribution peaks (see the details below). These problems can be ameliorated by employing "soft" training strategy ($\gamma = 1$) (Figure 9A). In this case, the maximum performance is higher (92.9%) and is achieved much more reliably albeit in noticeably higher number of training iterations. Similarly to the previous example, relatively low number of cells is sufficient to achieve this performance (Figure 9B). The performance is robust with respect to the readout noise (Figure 9C). An example of the evolution of the parameters of the classifier during "soft" training is shown in Figure 9D−I.

Analytical Description of Soft-Learning Performance. We have developed an analytical theory that describes the training and the resulting performance of the cell-based classifier in the limit of "soft" learning (see Supporting Information Section 1). This analytical description is exact in the case of infinitely "soft" learning and infinite number of cells. It is based on the assumption that at each training iteration the distribution of cells is changed by infinitely small amount, correspondingly requiring an infinite number of training iterations to achieve finite changes in cell distribution. Thus, the discrete iteration step can be replaced by continuous "time" t, and the evolution of the number of cells n_i with a given value m_i of genetic diversity parameter m_w in the course of training can be described by a differential equation

$$\frac{dn_i}{dt} = \lambda_i n_i - \frac{n_i}{N_c} \sum_k \lambda_k n_k$$

where N_c is the total number of cells (fixed) and λ_i is a "shaping factor" which depends on the distributions of the positive and negative training examples $w_\pm(x)$, m_i-dependent single cell GFP response functions $z(x; m_i)$ and the corresponding cell survival probabilities $p_\pm(z)$ (see Supporting Information Section 1). The solution of this equation approximates an ensemble average solution in the case of finite "softness", number of

Discrimination of two log-normal classes

Discrimination of a bimodal vs a unimodal class
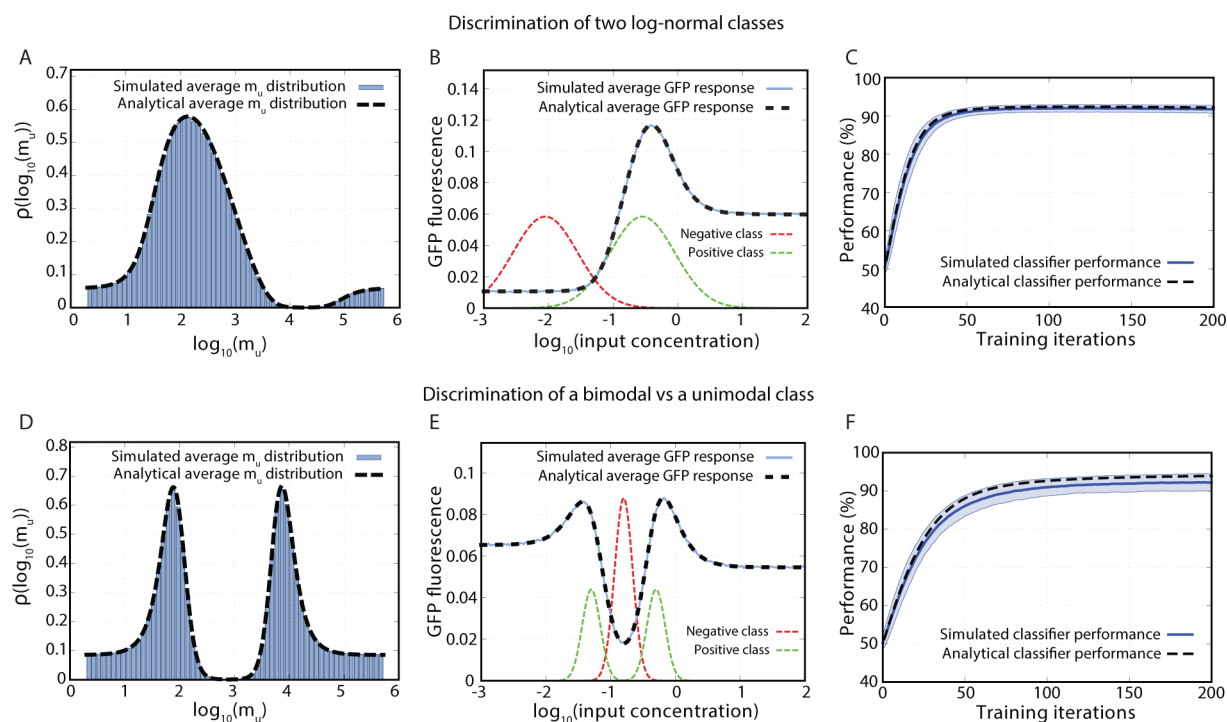
Figure 10. Comparison of the analytical theory with the simulation results for the case of soft-learning ($\gamma = 1$). (A−C) Discrimination of two log-normal classes. (D−F) Discrimination of a bimodal vs a unimodal class. (A, D) Ensemble average distribution of the genetic diversity parameter m_u calculated after 200 training iterations from 10^3 independent simulations (blue bars) vs the analytical prediction (black dashed line). (B, E) Ensemble average population-wide GFP responses calculated after 200 training iterations from 10^3 independent simulations (blue line) vs the analytical prediction (black dashed line). (C, F) Ensemble average classifier performance calculated from 10^3 independent simulations vs the analytical prediction; the simulation results are shown as mean ± standard deviation. All other simulation parameters are the same as in Figures 8D−I and 9D−I.

training steps (N), and finite number of cells by formally setting $t = N/2$. Figure 10 demonstrates the good agreement between the analytical solutions for the ensemble-averaged m_u distribution, population average GFP response, and the ensemble average classifier performance and the simulation results for "soft" learning with $\gamma = 1$. Note that the performance figures calculated analytically are consistently higher than the ensemble average performance figures calculated from the simulations (Figure 10C, F). This is largely due to the fact that the analytical approximation is based on asymptotic analytical solution which ignores the stochastic effects due to the finite number of iterations.

This analytical theory allows to quickly estimate the parameters for optimal training of the distributed cell population based classifier for a given classification problem. In comparison, the stochastic simulations necessary to estimate the same training parameters are significantly more computationally expensive. If necessary, the results of the analytical approximation can be confirmed by stochastic simulations.

Another important result that follows from the analytical approximation is that early stopping must be always used in order to maximize the classifier performance, even in the case of infinitely "soft" learning, since after large number of training iterations ($N \to \infty$) only the cells with the maximum λ_i survive. In most practical cases, it means that the cells with only one particular value of m_i survive, thus generally leading to poor classifier performance.

Summary and Discussion. In this paper, we introduced a conceptual design of a distributed classifier in the form of a population of microorganisms containing a strategically

constructed library of sensory gene circuits. We described an algorithm of training such a classifier by pruning the master population after iterative presentation of known positive and negative input−output examples. We characterized both numerically and analytically the performance of the proposed classifier based on a particular sensory gene circuit that is induced by the external chemical input within a certain range of concentrations and repressed outside of it. A library containing a broad distribution of such circuits with different sensitivities to the chemical input in individual cells within the master population can be constructed by randomizing the control sequences within the input genetic element of the sensing circuit. We demonstrated that after appropriate training the distributed classifier can achieve nearly optimal performance in solving the task of discriminating nonseparable input data sets.

In this theoretical study we have not addressed in detail several important issues that are likely to arise in the experimental implementation of the distributed classifier. One such issue is the specific procedure to retain the "good" cells and discard the "bad" ones. The most straightforward way to do this is to use a fluorescence-activated cell sorting (FACS). However, typical commercial FACS software allows one only to select cells deterministically with a measured fluorescent value (or a combination of multiple values) within a certain range— the process known as "gating"—rather than to sort cells with a certain probability based on their fluorescence levels. We envisage two ways to circumvent this problem. First, any smooth probability function can be approximated to a required precision by a step function by dividing the entire range of cell fluorescence on a sufficiently high number of bins. Cells with
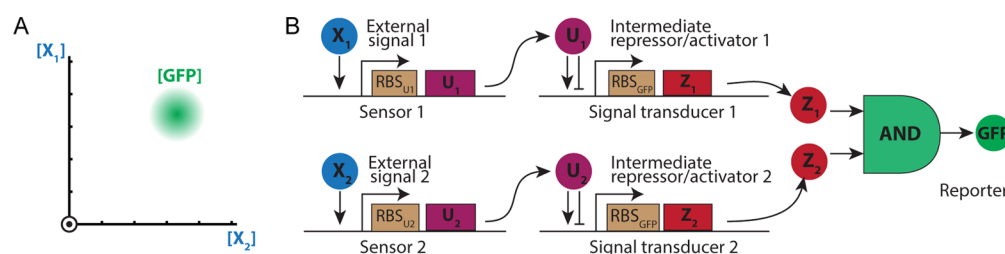
Figure 11. (A) Desired bell-shaped response of the multidimensional classification circuit. (B) The genetic circuit proposed for use in a distributed genetic classifier with multiple inputs per cell. Independent sensing and response functionalities are combined using an appropriate biological AND gate. The resulting response function of the entire two-promoter circuit is bell-shaped with respect to the inputs X_1 and X_2 for the relevant choice of parameters.

the fluorescence values falling within each bin can be independently sorted using standard FACS systems and later combined in proportions according to the corresponding probabilities of the smooth probability function. Alternatively, a probabilistic selection algorithm could implement directly by straightforward adaption of the FACS control software if the hardware programming interface is available. A potentially more interesting approach allowing for autonomous and adaptable training could be to engineer an additional synthetic gene circuit controlling cell growth based on the output signal, using for example one of well-characterized positive/negative selection systems.[41]

In this study, we assumed that the promoter strength parameters are initially distributed uniformly over a broad range; however, experimentally the distribution would likely be nonuniform. This nonuniformity may affect the ability to train the classifier to an arbitrary classification task. In order to estimate how sensitive the performance of the proposed classification system may be to nonuniformity of the initial distribution of parameters, we have calculated the performance of our distributed classifier starting with model distributions of varying degrees of nonuniformity (Supporting Information Section 4). Based on these calculations, we estimate that depending on the classification problem a moderate degree of nonuniformity can be tolerated. However, the more uniform the initial distribution is, the better the final performance of the trained classifier will be, so the design of a uniform library is one of the important considerations for the future experimental implementation of the classifier. Such a library may have to be designed and synthesized, preselected from a random library, or both (see the discussion in Supporting Information Section 4). Finally, we did not take into consideration the growth and division of cells that can affect the distribution of cells within the trained population if cells with different sensory circuit parameters differ in their doubling rates, for example, due to respective differences in metabolic burden exerted by these circuits.

The particular design of a distributed classifier presented here is suitable for classification of a scalar input (single chemical inducer X) only. Many real-world classification problems involve multidimensional inputs. The one-dimensional classifier described in this paper can be generalized to solve multidimensional problems. In the simplest case of multidimensional classification where each dimension can be classified independently, the problem can be trivially solved by a cell population classifier consisting of a mixture of cells capable of responding individually to just one input using the circuit described in Figure 1. However, such approach would fail for more complex classification problems when a multidimensional

distribution of positive or negative outcomes is not the direct product of corresponding one-dimensional distributions. These more complex problems can be solved using a classifier built with the cells endowed with circuits that are sensitive to multiple inputs. An example of such circuit design for a two-dimensional input is shown in Figure 11. In this design, the input signals are sensed separately by the corresponding two-stage modules similar to described above. The outputs of these two modules are then combined by a genetic AND gate. A number of circuits performing logical operations including AND have been developed and characterized recently.[48−50] Similarly to the one-dimensional circuit the output of this circuit is a two-dimensional bell-shaped function of the two inputs (Figure 11A). The parameters of both sensory circuits can be randomized as before. These multidimensional classifiers can be trained and the performance can be characterized in the same way as in the case of the one-dimensional classifier.

From synthetic biology perspective, our modeling study opens an intriguing possibility to engineer genetically diversified microbial populations to solve classification tasks which are difficult or impossible to solve within a single microbial cell. Such approach is known in machine learning theory where it was proven that consensus classifiers made of appropriately combined weak classifiers can achieve high performance.[51,52] We anticipate that beyond conceptual academic interest, autonomous cell population-based classifiers can have biotechnological and medical applications. The proposed circuit and its training algorithm could potentially be used to facilitate biosensor design. An autonomous classifier could directly produce a biologically relevant response, for example a drug or a signaling molecule can be synthesized *in situ* when the measured input concentration falls within or outside an optimal range. Such autonomous systems capable of responding to a complex input can be used e.g. to control bioreactors or as prosthetic control systems for use in living organisms. On a more general level, our findings suggest that perhaps the genetic and phenotypic diversity found in many natural populations,[53,54] along with other potential survival benefits[55] can play an important role in forming a decentralized "social intelligence"[15,56] capable of solving complex computational tasks in a noisy and unpredictable environment.

■ ASSOCIATED CONTENT

Ⓢ Supporting Information

Analytical treatment of soft learning; performance of the classifier model on the problem of discriminating toxicity data; classifier model based on experimentally derived PRM promoter response function; effect of non-uniformity of m_u

distribution in "master population". This material is available free of charge via the Internet at http://pubs.acs.org.

■ AUTHOR INFORMATION

Corresponding Authors
*E-mail: rhuerta@ucsd.edu.
*E-mail: ltsimring@ucsd.edu.

Notes
The authors declare no competing financial interest.

■ REFERENCES

(1) Bishop, C. M. (2007) *Pattern Recognition and Machine Learning (Information Science and Statistics)*; Springer, New York.

(2) Viola, P., and Jones, M. (2001) Rapid object detection using a boosted cascade of simple features. *Proceedings of the 2001 IEEE Computer Society Conference on Computer Vision and Pattern Recognition 1*, 511−518.

(3) Sebastiani, F. (2002) Machine learning in automated text categorization. *ACM Comput. Surv. 34*, 1−47.

(4) Manning, C. D., Raghavan, P., and Schütze, H. (2008) *Introduction to Information Retrieval*; Cambridge University Press: Cambridge, Vol. *1*.

(5) Kononenko, I. (2001) Machine learning for medical diagnosis: History, state of the art, and perspective. *Artif. Intell. Med. 23*, 89−109.

(6) Goodman, M., Porter, C. A., Czelusniak, J., Page, S. L., Schneider, H., Shoshani, J., Gunnell, G., and Groves, C. P. (1998) Toward a phylogenetic classification of primates based on DNA evidence complemented by fossil evidence. *Mol. Phylogenet. Evol. 9*, 585−598.

(7) Rabiner, L., and Juang, B.-H. (1993) *Fundamentals of Speech Recognition*; Prentice Hall, Upper Saddle River, NJ.

(8) Huerta, R., and Elkan, C. (2013) Nonlinear support vector machines can systematically identify stocks with high and low future returns. *Algorithmic Finance 2*, 3−43.

(9) Chan, P., and Stolfo, S. (1998) Toward scalable learning with non-uniform class and cost distributions: A case study in credit card fraud detection. *Proceedings of the Fourth International Conference on Knowledge Discovery and Data Mining*, 168.

(10) Witten, I. H., Frank, E., and Hall, M. A. (2011) *Data Mining: Practical Machine Learning Tools and Techniques*; Morgan Kaufmann, Burlington, MA.

(11) Maass, W., Natschläger, T., and Markram, H. (2002) Real-time computing without stable states: A new framework for neural computation based on perturbations. *Neural Comput. 14*, 2531−2560.

(12) Jaeger, H., and Haas, H. (2004) Harnessing nonlinearity: Predicting chaotic systems and saving energy in wireless communication. *Science 304*, 78−80.

(13) Ptashne, M. (1986) *A Genetic Switch: Gene Control and Phage Lambda*; Blackwell Scientific Publications, Palo Alto, CA.

(14) Rangel, A., Camerer, C., and Montague, P. R. (2008) A framework for studying the neurobiology of value-based decision making. *Nat. Rev. Neurosci. 9*, 545−556.

(15) Couzin, I. D. (2009) Collective cognition in animal groups. *Trends Cogn. Sci. 13*, 36−43.

(16) Amit, D. J. (1992) *Modeling Brain Function: The World of Attractor Neural Networks*; Cambridge University Press, Cambridge, New York.

(17) Haykin, S. (1994) *Neural Networks: A Comprehensive Foundation*, 1st ed.; Prentice Hall PTR: Upper Saddle River, NJ.

(18) Eason, D. D., Cannon, J. P., Haire, R. N., Rast, J. P., Ostrov, D. A., and Litman, G. W. (2004) Mechanisms of antigen receptor evolution. *Semin. Immunol. 16*, 215−226.

(19) Palmer, E. (2006) The T-cell antigen receptor: A logical response to an unknown ligand. *J. Recept. Signal Transduction 26*, 367−378.

(20) Farmer, J. D., Packard, N. H., and Perelson, A. S. (1986) The immune system, adaptation, and machine learning. *Phys. D (Amsterdam, Neth.) 22*, 187−204.

(21) Bersini, H., and Varela, F. J. (1991) *Parallel Problem Solving from Nature*; pp 343−354, Springer, Heidelberg, Berlin.

(22) Dasgupta, D. (1999) *An Overview of Artificial Immune Systems and Their Applications*; Springer, Heidelberg, Berlin.

(23) Schapire, R. E. (1990) The strength of weak learnability. *Mach. Learn. 5*, 197−227.

(24) Broomhead, D. S. and Lowe, D. (1988) Radial basis functions, multi-variable functional interpolation, and adaptive networks. *RSRE MEMORANDUM No. 4148*; Controller HMSO, London.

(25) Mallat, S. (1999) *A Wavelet Tour of Signal Processing*; Academic Press, New York.

(26) Pfleger, B. F., Pitera, D. J., Smolke, C. D., and Keasling, J. D. (2006) Combinatorial engineering of intergenic regions in operons tunes expression of multiple genes. *Nat. Biotechnol. 24*, 1027−1032.

(27) Wang, H. H., Isaacs, F. J., Carr, P. A., Sun, Z. Z., Xu, G., Forest, C. R., and Church, G. M. (2009) Programming cells by multiplex genome engineering and accelerated evolution. *Nature 460*, 894−898.

(28) Zelcbuch, L., Antonovsky, N., Bar-Even, A., Levin-Karp, A., Barenholz, U., Dayagi, M., Liebermeister, W., Flamholz, A., Noor, E., Amram, S., Brandis, A., Yofe, I., Jubran, H., and Milo, R. (2013) Spanning high-dimensional expression space using ribosome-binding site combinatorics. *Nucleic Acids Res. 41*, e98−e98.

(29) Isaacs, F. J., Hasty, J., Cantor, C. R., and Collins, J. J. (2003) Prediction and measurement of an autoregulatory genetic module. *Proc. Natl. Acad. Sci. U.S.A. 100*, 7714−7719.

(30) Lutz, R., and Bujard, H. (1997) Independent and tight regulation of transcriptional units in *Escherichia coli* via the LacR/O, the TetR/O, and AraC/I1-I2 regulatory elements. *Nucleic Acids Res. 25*, 1203.

(31) Cox, R. S., Surette, M. G., Elowitz, M. B. (2007) Programming gene expression with combinatorial promoters. *Mol. Syst. Biol. 3*.

(32) Salis, H. M., Mirsky, E. A., and Voigt, C. A. (2009) Automated design of synthetic ribosome binding sites to control protein expression. *Nat. Biotechnol. 27*, 946−950.

(33) Kudla, G., Murray, A. W., Tollervey, D., and Plotkin, J. B. (2009) Coding-sequence determinants of gene expression in *Escherichia coli*. *Science 324*, 255−258.

(34) Brewster, R. C., Jones, D. L., and Phillips, R. (2012) Tuning promoter strength through RNA polymerase binding site design in *Escherichia coli*. *PLoS Comput. Biol. 8*, e1002811.

(35) Carrier, T. A., and Keasling, J. (1999) Library of synthetic 5′ secondary structures to manipulate mRNA stability in *Escherichia coli*. *Biotechnol. Prog. 15*, 58−64.

(36) Wang, K. H., Oakes, E. S., Sauer, R. T., and Baker, T. A. (2008) Tuning the strength of a bacterial N-end rule degradation signal. *J. Biol. Chem. 283*, 24600−24607.

(37) Flynn, J. M., Levchenko, I., Seidel, M., Wickner, S. H., Sauer, R. T., and Baker, T. A. (2001) Overlapping recognition determinants within the ssrA degradation tag allow modulation of proteolysis. *Proc. Natl. Acad. Sci. U.S.A. 98*, 10584−10589.

(38) Zucca, S., Pasotti, L., Mazzini, G., De Angelis, M. G. C., and Magni, P. (2012) Characterization of an inducible promoter in different DNA copy number conditions. *BMC Bioinf. 13*, S11.

(39) Lee, S. K., and Keasling, J. D. (2005) A propionate-inducible expression system for enteric bacteria. *Appl. Environ. Microbiol. 71*, 6856−6862.

(40) Khlebnikov, A., Datsenko, K. A., Skaug, T., Wanner, B. L., and Keasling, J. D. (2001) Homogeneous expression of the PBAD promoter in Escherichia coli by constitutive expression of the low-affinity high-capacity AraE transporter. *Microbiology 147*, 3241−3247.

(41) Schaerli, Y., and Isalan, M. (2013) Building synthetic gene circuits from combinatorial libraries: screening and selection strategies. *Mol. BioSyst. 9*, 1559−1567.

(42) Fisher, R. A. (1936) The use of multiple measurements in taxonomic problems. *Ann. Eugenic. 7*, 179−188.

(43) Blumberg, M. S. (1957) Evaluating health screening procedures. *Oper. Res. 5*, 351−360.

(44) Loewe, S. (1953) The problem of synergism and antagonism of combined drugs. *Arzneimittelforschung 3*, 285−290.

(45) Yeh, P. J., Hegreness, M. J., Aiden, A. P., and Kishony, R. (2009) Drug interactions and the evolution of antibiotic resistance. *Nat. Rev. Microbiol. 7*, 460−466.

(46) Rosset, S., Zhu, J., and Hastie, T. (2004) Boosting as a regularized path to a maximum margin classifier. *J. Mach. Learn. Res. 5*, 941−973.

(47) Zhang, T., and Yu, B. (2005) Boosting with early stopping: Convergence and consistency. *Ann. Stat.*, 1538−1579.

(48) Wang, B., Kitney, R. I., Joly, N., and Buck, M. (2011) Engineering modular and orthogonal genetic logic gates for robust digital-like synthetic biology. *Nat. Commun. 2*, 508.

(49) Moon, T. S., Lou, C., Tamsir, A., Stanton, B. C., and Voigt, C. A. (2012) Genetic programs constructed from layered logic gates in single cells. *Nature 491*, 249−253.

(50) Shis, D. L., and Bennett, M. R. (2013) Library of synthetic transcriptional AND gates built with split T7 RNA polymerase mutants. *Proc. Natl. Acad. Sci. U.S.A. 110*, 5028−5033.

(51) Koltchinskii, V., and Panchenko, D. (2002) Empirical margin distributions and bounding the generalization error of combined classifiers. *Ann. Stat. 30*, 1−50.

(52) Zhang, Z., Liu, D., Dai, G., and Jordan, M. I. (2012) Coherence functions with applications in large-margin classification methods. *J. Mach. Learn. Res. 13*, 2705−2734.

(53) Nevo, E. (2001) Evolution of genome-phenome diversity under environmental stress. *Proc. Natl. Acad. Sci. U.S.A. 98*, 6233−6240.

(54) Avery, S. V. (2006) Microbial cell individuality and the underlying sources of heterogeneity. *Nat. Rev. Microbiol. 4*, 577−587.

(55) Fraser, D., and Kaern, M. (2009) A chance at survival: Gene expression noise and phenotypic diversification strategies. *Mol. Microbiol. 71*, 1333−1340.

(56) Jacob, E. B., Becker, I., Shapira, Y., and Levine, H. (2004) Bacterial linguistic communication and social intelligence. *Trends Microbiol. 12*, 366−372.